Assembly of b/HLH/z Proteins c-Myc, Max, and Mad1 with Cognate DNA: Importance of Protein−Protein and Protein−DNA Interactions†

Jianzhong Hu, Anamika Banerjee, and Dixie J. Goss*

Department of Chemistry, Hunter College, and Graduate Center of the City University of New York, New York, New York 10021

Received February 3, 2005; Revised Manuscript Received July 6, 2005

ABSTRACT: Among the best characterized of the transcription factors are the b/HLH/z proteins: USF, Max, Myc, and Mad. These proteins bind to the DNA E-box, a six base pair sequence, CACGTG. Max and Myc form a heterodimer that has strong oncogenic potential but can also repress transcription, while Mad and Max form a heterodimer that acts as a transcription repressor. We have used fluorescence anisotropy to measure protein−protein and protein−DNA affinity. The specific binding between MLP DNA and Max ($K = 2.2 \pm 0.5$ nM) is about 10-fold higher affinity than LCR DNA and about 100-fold higher than for a nonspecific DNA. USF has a similar binding affinity as Max to MLP DNA ($K = 15 \pm 10$ nM), but Max binds more tightly to LCR and nonspecific DNA. A series of oligonucleotides designated E-box, half-E-box, and non-E-box were constructed to examine the effects of DNA sequence. The binding results indicate that for Max protein most of the binding energy can be attributed to individual elements with little cooperativity among the two halves of the E-box. Further studies measured the equilibria for the entire thermodynamic cycle of monomer−dimer−DNA interactions. Surprisingly, the affinity of the Max monomer−DNA for the second monomer was greatly reduced (*K* for the first monomer in the nanomolar range and for the second monomer in the micromolar range). Looked at from the perspective of the Max protein, the binding of DNA to Max significantly reduces the affinity of the Max protein for the second monomer, whether the second monomer is Myc, Mad, or Max. These data suggest the importance of protein−protein interactions in assembly of a transcription initiation complex.

Max belongs to the basic helix−loop−helix leucine zipper (b/HLH/z)[1] class of mammalian proteins that bind to CACGTG sequences (E-box); this class includes USF (upstream stimulatory factor) (*1*, *2*) as well as c-Myc (*3*, *4*), TFEB (*5*, *6*), TFE3 (*7*), Mxil (*8*), Mix (*9*), MondoA (*10*), and Mnt (*11*), among others. The Myc gene is an oncogene, and overexpression of Myc occurs in a wide variety of human cancer cells (*12*−*16*). It is now well established that the deregulated expression of c-Myc plays a significant role in human cancer development. The Myc protein family including C-Myc, N-Myc, and L-Myc were indicated as direct regulators of gene expression. Although C-Myc, N-Myc, and L-Myc have different transcription activity in transformation, immortalization, blockage of cell differentiation, and induction of apoptosis (*6*, *17*−*19*), they have similar DNA binding properties. As basic helix−loop−helix leucine zipper proteins (b/HLH/z), the Myc family specifically binds the DNA sequence CACGTG (E-box) when dimerized with Max (*20*, *21*). The crystal structure of Myc-Max, as well as Mad-Max, bound to DNA has been determined and suggested that a head to tail pair of Myc-Max dimers may, in turn, form a heterotetramer capable of bridging distant E-boxes (*22*). Max protein not only is the partner of Myc but can heterodimerize with competing Mad family members or with Mnt. All of these heterodimers also bind E-boxes, as do Max homodimers. The basic helix−loop−helix leucine zipper (b/HLH/z) motif of these proteins is a conserved region of approximately 70 amino acids shown to be responsible for dimerization (*6*, *19*), and the conserved region at the N-terminal side is believed to be required for DNA binding to the protein dimer (*23*). A heptad repeat of leucine residues called the leucine zipper (Z or zip) at the C-terminus is required for high binding affinity and specificity of the protein for DNA and for dimerization stability (*1*, *6*, *24*, *25*).

After the identification of Max as a binding partner of different Myc proteins, including C-Myc, N-Myc, and L-Myc, there began a search for additional b/HLH/z dimerization partners. The search led to the discovery of the Mad family proteins Mad1, Mxi1, Mad3, and Mad4 as interaction partners of Max, and together these factors define the Myc/Max/Mad network (*26*, *27*). Later, two additional Max partners, Mnt and Mga, were found (*28*, *29*). Recently, the identification of Mlx, a Max-like protein that can het-

† This work was supported in part by NIH SCORE Grant (SO6 GM 60654) Research Centers in Minority Institutions Award RR-03037 from the National Center for Research Resources of the NIH supports infrastructure at Hunter College.

* To whom correspondence should be addressed. Tel: 212-772-5383. Fax: 212-772-5332. E-mail: dgoss@hunter.cuny.edu.

[1] Abbreviations: b/HLH/z, basic helix−loop−helix leucine zipper; USF, upstream stimulatory factor; DNA E-box, six base pair double-stranded DNA sequence CACGTG known as enhancer box; MLP, major late promoter; LCR, human β-globin locus control region; FITC, fluorescein isothiocyanate; TRITC, tetramethylrhodamine isothiocyanate; IPTG, isopropyl β-D-thiogalactopyranoside; HEPES, 4-(2-hydroxyethyl)-1-piperazineethanesulfonic acid; EDTA, ethylenediaminetetraacetic acid; DTT, dithiothreitol; PBS, phosphate-buffered saline.

10.1021/bi050206i CCC: $30.25
Published on Web 08/09/2005

erodimerize with Mad1, Mad4, and Mnt but not with the other Mad proteins nor with Myc or Max, has been reported (*9*, *30*). The most recent extensions of the network are the cloning of MondoA as an Mlx binding partner (*10*) and the identification of WBSCR14 that also interacts with Mlx (*31*). Both Max and Mlx are the central components of the network. It is possible that not all members of this network have been discovered and it will be of interest to detail additional components that may further expand the network.

Numerous studies have highlighted the importance of the Myc/Max/Mad network in regulating cell behavior (*27*). The formation of Myc-Max heterodimers is required for a number of biological activities such as transcriptional activation of promoters, cell transformation, proliferation, metabolism, and differentiation (*2*, *3*, *9*, *32*−*34*). Myc does not easily form homodimers, nor does the homodimer readily bind to DNA except at high concentrations under in vitro conditions (*23*, *35*, *36*). In contrast, Max can homodimerize and bind to the E-box of DNA. The Mad-Max heterodimer has the opposite function to Myc-Max and acts as a transcriptional repressor (*37*). Mad proteins inhibit reporter genes that are activated by Myc, interfere with transformation of rat embryo fibroblasts, block cell growth, inhibit cell proliferation, and prevent apoptosis (*27*, *38*). Although the function of Max homodimers is still not clear, formation of different Max heterodimers determines transcription activation or repression. Max protein plays a key role in the Myc-Max-Mad transcription regulation pathway.

While there have been a number of studies on the DNA sequence preferences of the b/HLH/z proteins, there have been very little quantitative data on protein−protein and protein−DNA interactions. An understanding of protein interactions with DNA is the first step in understanding the mechanism of action of this important biological process. In this work, we have investigated the binding of Max, Max-c-Myc, and Max-Mad1 to DNA oligomers containing the E-box and to other oligomers with various base substitutions. We have determined protein−protein interactions as well. The binding properties of Max to DNA are also compared to those of USF. USF has a biphasic binding mode representing a tetramer binding to two duplex DNA molecules (*1*, *25*). The results from direct fluorescence anisotropy titration measurements showed a single binding mode for Max binding to DNA that is attributed to a dimer−DNA interaction. Binding energy changes calculated from the equilibrium constants showed that the binding to the two halves of the E-box by each monomer in the dimer protein was nearly independent and had little cooperativity. Further analyses of the energy contributions from other steps in the assembly process suggest the relative importance of protein−protein and protein−DNA interactions. The equilibrium constants for the complete thermodynamic cycle for assembly of dimer DNA from monomer DNA have been determined. These data give insight into the assembly of the protein−DNA scaffolding and serve as the basis to investigate the effects of other members of this complex network.

MATERIALS AND METHODS

Protein Purification. The expression vectors Max/pET3a and c-Myc/pGex2T were obtained from S. K. Burley, Rockefeller University. The expression vector Mad1/pET30a was constructed using Mad cDNA (purchased from Open Biosystems, Huntsville, AL). The Max, Mad1, and c-Myc proteins were all expressed in *Escherichia coli* BL21-pLys cells containing the DE3 promoter. To obtain soluble proteins, Max consisted of amino acids 22−113, c-Myc consisted of amino acids 347−439, and Mad1 was the full-length protein. These constructs contained the functional b/HLH/z domains of the proteins. Cells containing pET-Max or pGEX-Myc were selected by colony selection and inoculated into 1 L of LB media with 50 μg/mL ampicillin. After being grown to 0.6 OD_{600}, the cells were induced with 1 mM isopropyl β-D-thiogalactopyranoside (IPTG) and further incubated for 6 h. Cells containing pET-Mad vectors were also selected by colony selection. Ten milliliters of transformed *E. coli* cells was inoculated into 1 L of LB media with 50 μg/mL kanamicin and grown to 0.6−0.8 OD_{600}. The cells were induced with IPTG and continued to grow for 6 h. The pellets were collected by centrifugation for 20 min and 6000 rpm and resuspended in HEPES buffer (pH 7.6) (for Myc PBS, pH 7.4, was used) with protease inhibitor cocktail and lysozyme. The cells were stored on ice for 1 h and then sonicated twice for 1 min with a 30 s interval between sonication. The supernatant was used for chromatography and purification of the proteins. For Mad1 and c-Myc, the pellets were also saved for treatment of inclusion bodies.

The inclusion bodies for Mad1 were washed twice with 10 mL of 20 mM HEPES buffer (pH 7.6) containing 1% Triton X-100 followed by centrifugation at 18000 rpm for 30 min at 4 °C. The pellet (inclusion bodies) was dissolved in 2 mL of 50 mM HEPES buffer, pH 7.6, 6 M guanidine hydrochloride, and 25 mM DTT and incubated for 1 h at 4 °C. Insoluble material was removed by centrifugation (18000 rpm, 10 min), and the supernatant was diluted into 20 mL of cold 50 mM HEPES, pH 7.6.

The inclusion bodies for c-Myc were washed as described above for Mad1. The pellet was dissolved in 10 mL of PBS buffer, pH 7.4, containing 1% Triton X-100 and incubated overnight with gentle stirring. Insoluble material was removed as described above, and the supernatant was diluted into 20 mL of cold 20 mM PBS, pH 7.4.

Max was purified by HiTrap SP ion-exchange chromatography using the same protocol as described elsewhere (*21*, *25*). c-Myc was purified by GST affinity chromatography (Amersham Biosciences) using 20 mM PBS, pH 7.4, as the wash buffer and 50 mM glutathione and 200 mM Tris-HCl, pH 8.5, as the elution buffer. Mad1 was purified on a Ni^{2+}-His trap affinity column (Novagen). Depending on the concentration of protein in the sample and the His-bind resin capacity, the proper volume of resin was packed under gravity flow. Resin was washed with 10 volumes of binding buffer (0.5 M NaCl, 20 mM Tris-HCl, 5 mM imidazole, pH 7.9), and the protein samples were loaded onto the column. The column was washed with additional binding buffer and 3−10 volumes of wash buffer (0.5 M NaCl, 60 mM imidazole, 20 mM Tris-HCl, pH 7.9), and the protein was eluted with the same buffer containing 1 M imidazole. The protein fractions were collected, extensively dialyzed in HEPES buffer, pH 7.6, purity analyzed by SDS−PAGE, and concentrated, and the concentrations were determined using a Bio-Rad protein assay kit (Bio-Rad Laboratories, Hercules, CA).

Chart 1

Oligonucleotides	DNA sequences (complementary strand not shown)
16-mer MLP	5'TAGGC**CACGTG**ACCGG3'
16-mer LCR	5'TAG*AC***CAC*CTG***AC*T*G**GG3'
16-mer mLCR	5'TAGGC**CAC*CTG***CC*T*C**G3'
21-mer E-Box	5'GTGTAGGC**CACGTG**ACCGGGT3'
21-mer Half-Ebox	5'GTGTAGGC**CA*G*GTG**ACCGGGT3'
21-mer Non-Ebox	5'GTGTAGGC**CA*GC*TG**ACCGGGT3'

Fluorescent Labeling of Max Protein. The N-terminus of Max protein was labeled with tetramethylrhodamine 5-isothiocyanate (TRITC). Because TRITC reacts only with uncharged primary amines, under mild conditions, the N-terminus of Max was labeled. Max protein concentration was adjusted to ~1.0 mg/mL in 50 mM HEPES buffer (pH 7.6) and a total volume of 5.0 mL. One hundred microliters of TRITC dissolved in anhydrous DMSO (1.5 mg/mL) was added per milliliter of protein solution. The protein−dye mixture was incubated overnight in the dark at 4 °C with continuous gentle agitation. Labeled protein was separated from free rhodamine compounds by Sephadex G-15 gel filtration eluted with HEPES buffer. The collected fractions were concentrated with Centricon YM filters (Amicon Corp.) by centrifugation for 6 h at 4000 rpm. The final protein concentration and fluorophore/protein (F/P) ratio were determined by measuring absorbance at 280 and 555 nm. The following formula was used to obtain F/P ratios:

$$A_{\text{protein}} = (A_{280} - A_{555})\text{CF}$$

where $\text{CF} = (A_{280\ \text{free dye}})/(A_{555\ \text{free dye}}) = 0.30$ for TRITC and [protein] $= A_{\text{protein}}/(1.4\ \text{mg/mL})$, and the F/P ratio was calculated using $\epsilon = 93000$ for TRITC.

The site of protein labeling was confirmed by enzymatic digestion. Approximately 90% of the protein was labeled (1 dye/monomer). Labeling at sites other than the N-terminus was not detected.

DNA Oligonucleotides. DNA binding was measured using synthetic oligonucleotides purchased from GeneLink (Hawthorne, NY). The 21- or 16-bp oligonucleotides used in this study contained the sequence derived from the adenovirus major late promoter (MLP) containing the E-box (CACGTG). Sequences with three bases that are different from the MLP sequence are based on the human globin locus control region (LCR) transcription complex which contains the USF binding site. A modified LCR (mLCR) sequence with three other mutations and a base mismatch in the E-box was also used. Three 21mer oligonucleotides were used to measure the difference in binding for variations in the E-box sequence. Sequences of the oligonucleotides used are listed in Chart 1. The oligonucleotides were hybridized together to form double-stranded DNA before titrations. Equal concentrations (10−20 μM) of labeled oligonucleotides and their unlabeled complements were dissolved in nuclease-free water, heated to 75−80 °C for 30 min, and allowed to cool slowly overnight. The DNA oligonucleotide was purchased either as an unlabeled oligonucleotide (and its complement) or with a 5′ fluorescein isothiocyanate derivative.

Fluorescence Methods. Fluorescence polarization and anisotropy have been used extensively to monitor protein−protein and protein−DNA interactions (cf. ref *39* and references cited therein). For globular proteins, the rotational correlation time, ϕ, is approximately related to the molecular weight of the protein (M) and is given by the equation:

$$\phi = (\eta M/RT)(\bar{\nu} + h) \quad (1)$$

where ν is the specific volume of the protein, R is the gas constant, T is the temperature, η is the viscosity, and h is the hydration, typically 0.2 g of H_2O/g of protein, although in practice usually somewhat larger due to the nonspherical shape of proteins. From the above equation the predicted anisotropy can be related to the molecular weight for each species by

$$r_{\text{obs}} = \frac{r_0}{1 + (\tau/\phi)} = \frac{r_0}{1 + [\tau/(\eta M/RT)](\bar{\nu} + h)}$$

where r_{obs} is the observed anisotropy, r_0 is the anisotropy in the absence of ligand, τ is the fluorescence lifetime, and other parameters are as defined in eq 1.

For interactions where the fluorescence intensity does not change, r_{obs} is related to $\sum c_i r_i$, where c_i and r_i represent the concentration and anisotropy of the ith species, respectively.

The equation used for data fitting to obtain monomer−dimer dissociation equilibrium constants was (*40*, *41*)

$$r_{\text{obs}} = r_{\text{min}} + \frac{(r_{\text{max}} - r_{\text{min}})}{2[\text{Max}]}\{b - \sqrt{b^2 - 4[\text{Myc}][\text{Max}]}\}$$

$$b = K_{\text{D}} + [\text{Myc}] + [\text{Max}]$$

where r_{obs} is the observed anisotropy for any point in the titration curve, r_{max} is the maximum observed anisotropy, r_{min} is the minimum observed anisotropy, [Myc] and [Max] are the equilibrium protein concentrations, and K_{D} is the dissociation equilibrium constant. Theoretically, once r_{min} and r_{max} are known, any single point will give the K_{D} value; therefore, there is considerable redundancy in the data collection. The r_{min} values are determined from low concentration of protein, and the r_{max} value is the value at the end of the titration. Usually titrations with two different starting concentrations of proteins are fit simultaneously, and r_{max} is fit as another variable. This reduces any errors from choosing the wrong end point of the curve.

Protein Dimer Binding to DNA Oligonucleotides. Fluorescently labeled DNA oligonucleotides were titrated with unlabeled protein. The resulting anisotropy change was used to calculate the dissociation equilibrium constant according to equations described previously (*40*, *42*). Fluorescence measurements were performed with a SPEX τ2 spectrophotometer, and data were fit with the KaleidaGraph data analysis program.

Oligonucleotide concentrations were 15−50 nM. Titrations were carried out in 25 mM HEPES−KOH buffer, pH 7.6, containing 50 mM KCl, 10 mM DTT, 5 mM $MgCl_2$, and 0.5 mM EDTA for heterodimer titrations; Myc or Mad concentrations were in 5−10-fold excess of Max. Max was preincubated with the Myc or Mad protein prior to titration.

RESULTS AND DISCUSSION

The binding affinity of Max protein for LCR and MLP DNA oligonucleotides was measured in order to compare the binding with USF protein and structural data. The MLP

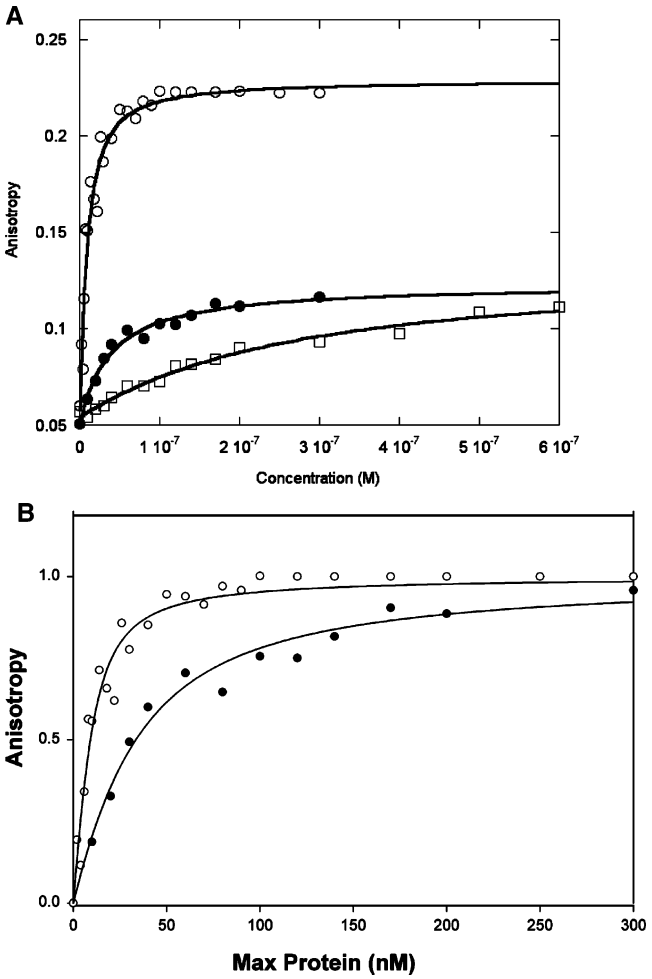

FIGURE 1: (A) MLP DNA oligonucleotide (○), LCR DNA oligonucleotide (●), and mLCR DNA oligonucleotide (□) titrated with Max protein. The concentration of MLP was 20 nM; the concentrations of LCR and mLCR were 100 nM. Anisotropy change was shown as the *Y* value by increasing the Max protein concentration (*X* value). The temperature was 22 °C. The titration curves indicate stronger binding affinity for MLP than LCR. (B) Normalized binding of Max protein to MLP (○) and LCR (●) DNA oligonucleotides. The normalized values represent the fraction bound. Experimental conditions are as described for panel A.

Table 1: Equilibrium Binding Constants and Specificities of USF and Max with DNA

oligos (12mers)	K_{eq} (nM) USF	specificity	K_{eq} (nM) Max	specificity
MLP	15 ± 10	1090	2.2 ± 0.5	104
LCR	3133 ± 570	3.0	33.3 ± 7.7	9.6
mLCR	9820 ± 2680	1.0	230 ± 10	1.0

sequence was also used in the X-ray crystallographic structure determination of Max_2−DNA (*21*). Our previous studies of USF (*25*) indicated that a biphasic mode of binding occurred with a high degree of specificity for MLP compared to LCR or mLCR (orginally designated nonspecific DNA). The titration data shown in Figure 1 demonstrate that there are significant differences in the binding affinity of Max protein to MLP and LCR DNA. The specific binding between MLP DNA and Max is about 10-fold higher affinity than LCR DNA and about 100-fold tighter binding than for the mLCR sequence (Table 1). An interesting observation is that the final anisotropy of the bound DNA is considerably higher for the MLP DNA than for mLCR or LCR DNA (0.223 ± 0.01 and 0.116 ± 0.01, respectively). In the case of mLCR DNA, this may be partially due to the contribution of free labeled DNA. Because of the low binding affinity, it is difficult to saturate the DNA with protein. The final anisotropy was extrapolated from the binding curve and obtained as a fitting parameter. Using the same final anisotropy obtained for MLP DNA in the fitting could not adequately fit the data. The final anisotropy is lower for the nonspecific sequences. This suggests that the binding mode may lock the DNA into a more rigid conformation for the specific binding, allowing less rotation even at the terminus where the fluorescent label is attached. This could be accomplished by interactions outside the E-box binding region such as a hydrogen bond between an amino acid in the loop region of the protein and the flanking sequence of the DNA (*43*). It is also possible that there could be a charge interaction between an amino acid side chain such as Lys 57 and a residue in the flanking sequence. We have determined the pH dependence of the binding between pH 6.5 and pH 8.5 (data not shown). No significant changes in binding affinity as a function of pH were found. This would indicate that if a charged residue is involved, it does not have a p*K* near this pH range. Cave et al. (*44*) used NMR to study Pho4 b/HLH domain binding to E-box and nonspecific DNA. They concluded that there was little difference in protein backbone dynamics but that the protein may slide along the nonspecific target sequence. Such motion would contribute to a lower overall anisotropy for LCR and mLCR DNA binding.

The data in Figure 1 show a single binding mode for Max binding to DNA. The Max−DNA binding profiles indicated Max dimer binding to DNA and did not show a biphasic binding mode which has been observed with USF (25). USF, another b/HLH/Z protein, recognizes the same E-box sequence and binds as two dimers (homotetramer) to two duplex DNA molecules (or to two E-box sites on the same DNA which forms a loop). A comparison of the binding constants (Table 1) for Max and those of USF to MLP DNA shows that both bind with similar affinities (nanomolar) but USF has 10 times higher specificity of binding to MLP DNA than Max. Max binds both LCR and mLCR DNA more tightly than USF. The lower specificity of binding of Max to MLP DNA suggests differences in transcriptional regulatory functions between Max and USF. USF is believed to mediate DNA looping by binding to two E-box sites in a biphasic mode: the first USF dimer binding tightly to one E-box and a second dimer binds with 10-fold lower affinity to the second E-box. The formation of a DNA loop is thought to be necessary for stimulating transcription and requires a high degree of specificity of USF for DNA. On the other hand, Max is known to activate transcription by binding to Myc oncoprotein and to cause repression of Myc transcriptional activities in high concentrations by forming homodimers which are believed to block the E-box site. Max function may be more important in determining the formation of heterodimers than in the selection of DNA.

It has been shown that Max binds as a dimer to the E-box with each monomer interacting with one-half of the E-box (*21*). Similar binding is observed for the Myc-Max and Max-Mad1 heterodimer binding to E-box DNA (*22*). The series of oligonucleotides described in Materials and Methods as E-box, half-E-Box, and non-E-Box was constructed to

Table 2: Dissociation Constants (K_d) and ΔG for Protein Binding with Different Oligonucleotides

oligos (21mers)	Max_2 K_d (nM)	ΔG (kJ)	Max-c-Myc K_d (nM)	ΔG (kJ)	Max-Mad K_d (nM)	ΔG (kJ)
E-box	19.2 ± 4.4	43.3 ± 0.5	90.5 ± 25.4	39.6 ± 0.8	192 ± 48	37.7 ± 0.6
half-E-box	48.7 ± 8.3	41.1 ± 0.3	229 ± 35	37.3 ± 0.3	315 ± 83	36.5 ± 0.6
non-E-box	87.0 ± 20	39.0 ± 0.4				

examine the contribution of each half of the E-box to dimer binding affinity and stability. The non-E-box has only altered the two central bases and is still considered an E-box, however lacking two essential interactions (see below). Table 2 shows the equilibrium dissociation constants and corresponding ΔG values for the Max homodimer and the two heterodimers. These oligonucleotides also allow an evaluation of the extent to which there is cooperativity between the two E-box half-sites. The cooperativity between these two sites can be determined by the free energy differences in binding. For binding of two different ligands to a macromolecule, Weber (*45*) has proposed a simple procedure for depicting the heterotropic free energy of interaction, the "coupling energy". This quantity indicates by how much and in what direction there is error in estimating the overall free energy of binding from knowledge of the separate binding free energies. At equilibrium, the free energy change for specific binding is given by

$$\Delta G_{\mathrm{E-box}} = -RT \ln K_1$$

$$\Delta G_{\mathrm{half-E-box}} = -RT \ln K_2$$

$$\Delta G_{\mathrm{non-E-box}} = -RT \ln K_3$$

Consider binding by each half-site and determine the cooperativity:

$$\Delta G_{\mathrm{non-E-box}} = -RT \ln K_3 = 2\Delta G_{\mathrm{nonspecific}} \text{ (for each half-site)} \quad (1)$$

$$\Delta G_{\mathrm{half\ -E-box}} = -RT \ln K_2 = \Delta G_{\mathrm{E-site}} + 2\Delta G_{\mathrm{nonspecific}} \quad (2)$$

where $\Delta G_{\mathrm{E-site}}$ is the additional free energy due to the specific site.

$$\Delta G_{\mathrm{E-box}} = -RT \ln K_1 = 2\Delta G_{\mathrm{nonspecific}} + 2\Delta G_{\mathrm{E-site}} \quad (3)$$

These equations partition the free energy to that associated with the optimum E-box sequence and that associated with the "non-E-box" sequence which retains some binding affinity.

Looked at from the perspective of DNA, one can determine two $\Delta\Delta G$ functions. These functions determine how much binding at one site can be said to influence the binding at the second site. These functions are

$$\Delta\Delta G_{3,2} = (3) - (2) \quad \text{and} \quad \Delta\Delta G_{2,1} = (2) - (1)$$

This $\Delta\Delta G$ represents the additional free energy for the specific site (half-E-box). The extent to which these two numbers are different indicates cooperativity, noncooperative or anticooperative binding. The binding curves for Max_2−DNA are shown as Figure 2. Mad-Max and Myc-Max binding to oligonucleotides is shown as Figures 3 and 4, respectively. A comparison of the equilibrium values in Table 2 shows that for the Max homodimer $\Delta\Delta G_{3,2} = 2.2$ kJ and $\Delta\Delta G_{2,1} = 2.0$ kJ. There is a 0.2 kJ/mol ΔG difference between these two numbers, showing that there may be a slight cooperativity in the Max binding with DNA to the two sites. Thus binding to one site only slightly, if at all, stabilizes the second binding site. However, the effects are very small, and binding can be interpreted to be independent within experimental error. This indicates that the affinity of the second monomer for DNA, at least in the case of Max, is not greatly affected by the presence of Max already bound at one-half the E-box. Each half of the E-box contributes 2−3 kJ/mol to the binding free energy. However, it should

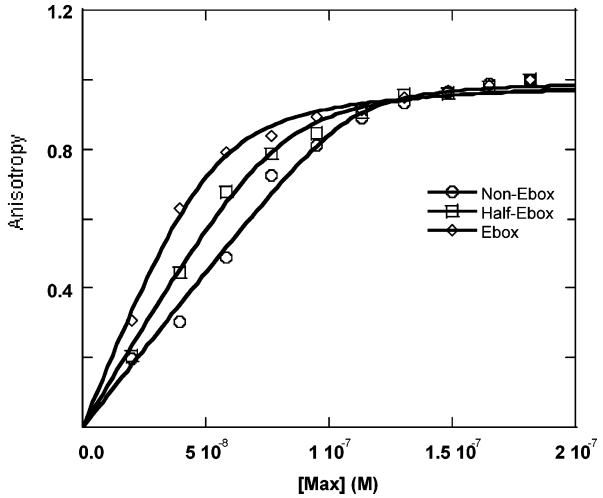

FIGURE 2: Anisotropy change for the interaction between Max protein and three different oligonucleotides. The concentrations of E-box (◇), half-E-box (□), and non-E-box (○) oligonucleotides were 50 nM. The temperature was 21 °C. The base sequences for the oligonucleotides are given in Materials and Methods. The equilibrium constants obtained from the anisotropy change are listed in Table 2.

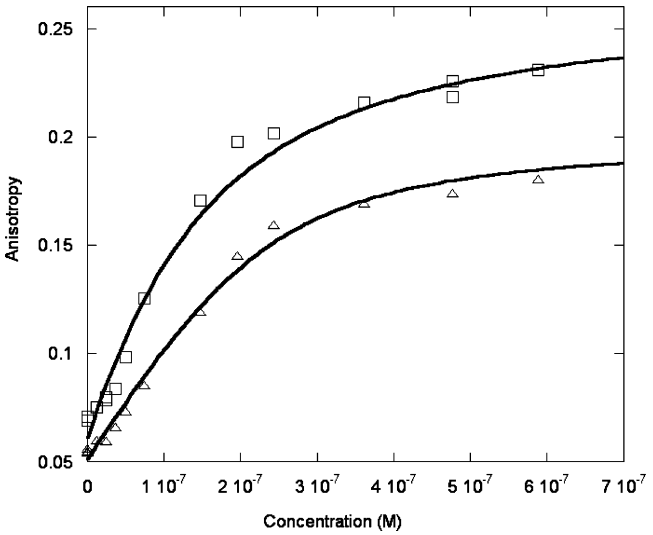

FIGURE 3: Anisotropy change for the interaction between Myc-Max protein and E-box (□) and half-E-box (△) oligonucleotides. The experimental conditions are the same as for Figure 2.

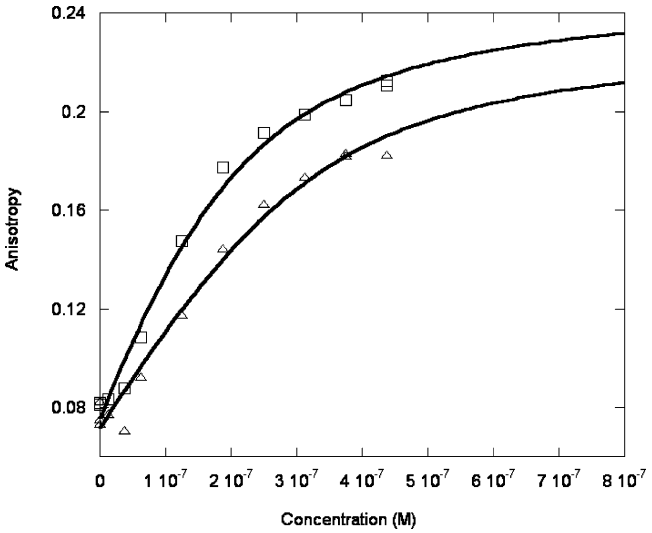

FIGURE 4: Anisotropy change for the interaction between Mad-Max protein and E-box (□) and half-E-box (△) oligonucleotides. The experimental conditions are the same as for Figure 2.

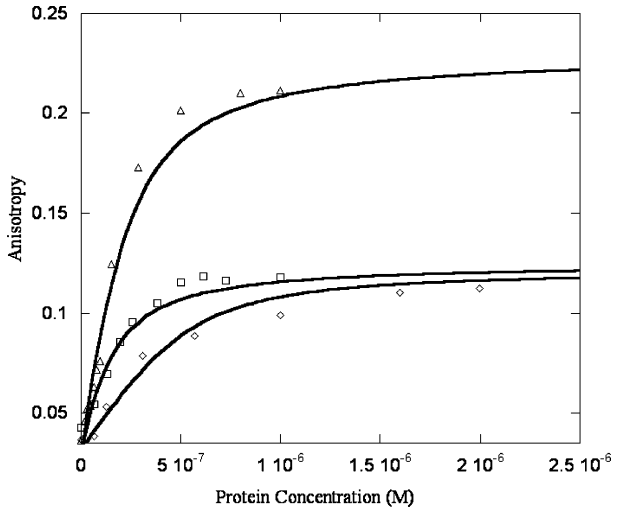

FIGURE 5: Dimerization of Max-Max (◇), Myc-Max (□), and Mad-Max (○). Max was labeled with TRITC. Labeled Max (100 nM) was titrated with increasing concentrations of unlabeled Max, Myc, or Mad. For these experiments, GST was enzymatically removed from Myc. The temperature was 20 °C. The larger anisotropy change for Mad is attributed to the larger molecular mass.

be emphasized that this partitioning of the free energy relates to the effects of DNA sequence. The half-E-box and non-E-box oligonucleotides remove specific interactions. An H-bond between a conserved Arg in the basic region and a C═O in the base of C is removed in the case of half-E-box and the second corresponding interaction is removed in the case of non-E-box DNA. The protein−protein interactions have significant contributions to the overall binding energy.

Titration experiments have been performed with Max-c-Myc and Max-Mad1 heterodimers to detect the free energy contribution of their interactions with the same E-box, half-E-box, and non-E-box DNA sequences. The results showed the similarity in binding between these two heterodimers but very different binding from the Max homodimer (Table 2, Figures 3 and 4). For the heterodimers, the free energy differences between nonspecific binding and E-box binding were much larger than for the Max homodimer interacting with DNA. We were unable to accurately measure binding of the heterodimers to the non-E-box sequences. These results support the hypothesis that, in the Myc/Max/Mad network, Max contributes more to the high binding affinity to the DNA; however, recognition of DNA sequences is more likely contributed by Max's partner, Myc or Mad. These results also support previous studies of binding preference that suggest Myc-Max heterodimers bind only a subset of the sites bound by Max homodimers, due to a differential recognition of the flanking sequences (*46*−*48*). O'Hagan et al. (*47*) argue that the basic regions of Myc and Mad are not functionally equivalent in oncogenesis; however, James and Eisenman (*49*) suggest that Myc and Mad have identical DNA binding activities but the in vivo functions are different, presumably due to other factors. It will be interesting to determine the effects of other proteins on these interactions.

To determine monomer−dimer equilibrium constants, Max was fluorescently labeled at the N-terminus. The labeling site was confirmed by protein digestion. Max protein was labeled with fluorescein or TRITC; both dyes react covalently with uncharged amines. By using low pH, the N-terminus is the only site labeled. These fluorescent probes allow excitation in the 520−640 nm range, which is well away from protein or DNA absorbance, thus minimizing inner-filter and other artifacts. Because anisotropy depends on the rotational relaxation time, an increase in molecular weight, such as dimer formation, is expected to increase the anisotropy. If there is no change in fluorescence lifetime and the limiting anisotropy is not reached, the change is directly proportional to the molecular weight change. Thus when labeled Max is titrated with unlabeled Max, Myc, or Mad, an increase in fluorescence anisotropy is expected. Figure 5 shows the anisotropy change observed. The larger anisotropy change for Mad (left curve) is due to the larger molecular weight of the heterodimer. The Max homodimer has a molecular mass of ∼20 kDa, the Myc-Max heterodimer is ∼23 kDa with GST removed from Myc, and Mad-Max is ∼42 kDa. Tetramer formation of Myc-Max as reported from X-ray crystallography (*22*) would result in substantially higher values for the anisotropy. The stoichiometry of these reactions was determined by analysis of the anisotropy, which is related to the molecular mass as described above. When Max was titrated with a larger species (Mad or GST-Myc), the anisotropy was substantially higher. In addition, nondenaturing gel electrophoresis (data not shown) was consistent with dimer formation. There was no evidence of tetramer formation under these experimental conditions. Table 3 shows the binding constants obtained from fitting the anisotropy data.

Table 3: Binding Constants (K_d) for Protein−Protein Interaction between Max-Max, Max-c-Myc, and Max-Mad Proteins

Max-Max (nM)	Max-c-Myc (nM)	Max-Mad (nM)
680 ± 44	176 ± 12	320 ± 25

Recently Park et al. (*50*) determined the kinetic rate constants for Myc-Max and Max-Max binding to an E-box oligonucleotide by gel electrophoresis. From the kinetic data, they obtained equilibrium constants for dimer binding to DNA and monomer−dimer equilibria. Park et al. (*50*) equilibrium constants for dimer binding were similar to our results for Myc-Max binding to DNA (K_{eq} = 145 nM; our data, 90.5 nM). The data presented here, however, for Max dimer binding show an almost 7-fold tighter binding to DNA

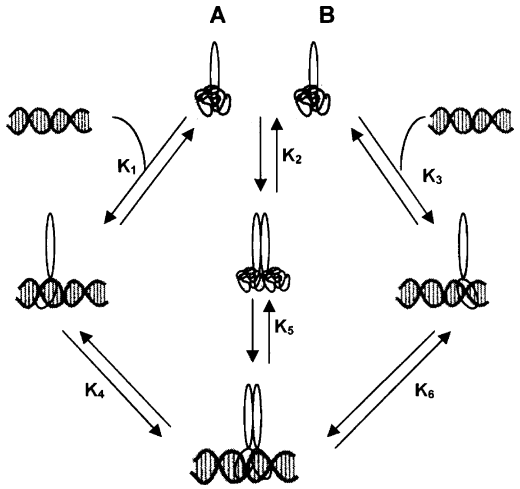

FIGURE 6: Schematic diagram of monomer, dimer, and DNA interactions.

compared to the values obtained by Park et al. Similarly, Park et al. show lower monomer−dimer affinity for Myc−Max interaction (78 μM compared to 176 nM). The differences in monomer−dimer equlibria may result from slightly different experimental conditions or from the difficulty in obtaining monomer−dimer values from gel electrophoresis experiments.

Assembly of the dimer−DNA complex for the Myc/Max/Mad proteins can be described by the cartoon shown in Figure 6. This cartoon represents the case for heterodimer−DNA formation where A and B are different monomers. The unstructured monomers interact with DNA (K_1, K_3) or each other (K_2). The monomer pathway (K_1, K_4 or K_3, K_6) predicts the sequential addition of the second monomer. (For steps K_4 and K_6, the second monomer is not shown.) The dimer binding pathway (K_2, K_5) is also included. In the case of homodimer formation, A and B are identical and therefore $K_1 = K_3$ and $K_4 = K_6$, thus simplifying the scheme. The protein monomer−dimer equilibrium (K_2) is listed in Table 3. Dimer binding to DNA was also determined. For homodimers, it has been reported (*35*, *35*, *51*) that neither Myc nor Mad binds DNA very well. Consequently, if a solution is composed of Max and an excess of either Myc or Mad as described in Materials and Methods, the predominant species will be Myc_2 and Max-Myc. Using Myc-Max as an example, data indicate that the Myc-Max monomer−dimer equilibrium constant is around 0.2 mM and the Myc-Max−DNA binding is around 5 nM. There is one important observation, however, that will allow us to determine the dimer−DNA equilibrium constant and that is the fact that Myc_2 binds DNA poorly and that Myc forms a homodimer only weakly. We find that by having Max at low nanomolar concentrations and Myc at low micromolar concentration, essentially all of the Max is in the desired Myc-Max complex. At these low concentrations, there is negligible Max dimer present.

Given the equilibrium data, assembly of dimer−DNA complexes must follow a monomer pathway because binding to DNA occurs in the nanomolar range and monomer−dimer association occurs in the micromolar range. Therefore, there is virtually no dimer present initially when DNA is titrated with protein, and the initial binding must be a monomer. A titration of DNA with low concentrations of Max, followed by Myc, yields the fluorescence titration curve shown in

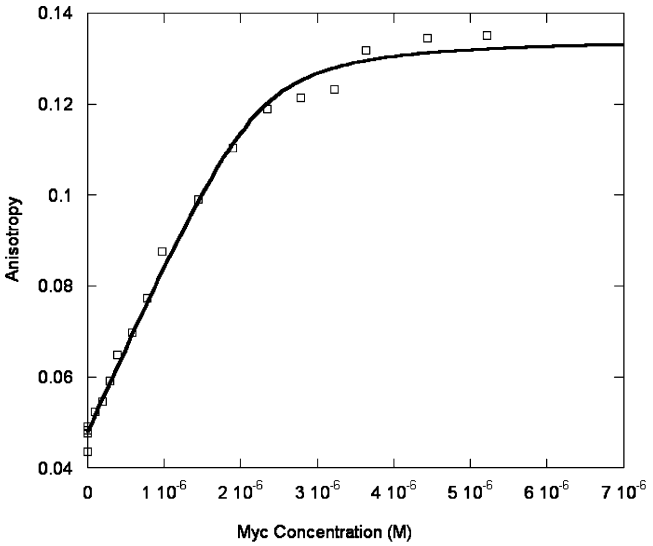

FIGURE 7: Titration of Max−DNA (50 nM) with increasing concentrations of Myc protein. The E-box oligonucleotide labeled with 5′ FITC was used for the titration. The temperature was 21 °C.

Figure 7. The K_{obs} is K_1K_4 in Figure 6 (monomer binding to DNA followed by second monomer binding) where

$$K_{obs} = [Myc][Max][DNA]/[Myc\text{-}Max{-}DNA]$$

$$K_1 = [Max][DNA]/[Max{-}DNA]$$

$$K_4 = [Max{-}DNA][Myc]/[Myc\text{-}Max{-}DNA]$$

Because of the low affinity of homodimeric Myc or Mad for DNA (*27*), binding of these monomers to DNA can be neglected. For all three proteins, K_1 will be the same because Max binds first and is the only monomer protein that has a significant affinity for DNA. The following expressions can be written:

$$K_{obsMax} = K_1K_{4Max}$$

$$K_{obsMyc} = K_1K_{4Myc}$$

$$K_{obsMad} = K_1K_{4Mad}$$

where K_{obs} is the experimentally determined equilibrium constant from the binding curve, K_1 is the monomer binding of Max to DNA, and K_4 is the sequential addition for each of the proteins as indicated. From these data one can obtain the relative affinity of Myc or Mad for Max−DNA (K_{4Myc}/K_{4Mad}).

The above relationships give three equations and four unknowns. However, we can use the thermodynamic cycle to write two additional expressions: $K_1 = K_{2Myc}K_{5Myc}/K_{4Myc}$ and $K_1 = K_{2Mad}K_{5Mad}/K_{4Mad}$. K_5, the dimer binding to DNA, was determined as described above for both Mad-Max and Myc-Max, and the monomer−dimer equilibrium, K_2, was determined for both proteins. By titration of a solution of labeled Max and excess DNA with either Myc or Mad, K_4 was measured, and using the above equations, K_1 was also obtained. Table 4 gives the relevant equilibrium values for the entire pathway. The values for K_1 obtained by using the Myc equilibrium constants and the Mad equilibrium constants

Table 4: Equilibrium Constants for Reactions in Figure 6[a]

protein	K_1 (K_3) (nM)	K_2 (nM)	K_4 (K_6) (μM)	K_5 (nM)
c-Myc	6.8 ± 1.6	176 ± 12	2.2 ± 0.1	84 ± 10
Mad	10.2 ± 1.8	320 ± 25	5.3 ± 0.2	168 ± 14
Max	8.1 ± 1.2	680 ± 44	2.1 ± 0.1	15 ± 2

[a] The values for K_1 are for the first Max monomer binding to DNA as calculated from data for the binding of the Myc, Mad, or Max hetero- or homodimer as described in Results and Discussion.

are different by less than a factor of 2. This redundancy gives good agreement in the final parameters.

On the basis of the equilibrium values obtained, the in vitro pathway during a titration follows a monomer pathway, which is consistent with kinetic data (*41*). The binding of Max monomer occurs at concentrations well below the formation of dimers. The pathway forms a thermodynamic cycle, and therefore the stability of the final complex will not depend on the pathway followed. These equilibrium data suggest that, at physiological conditions, most of the DNA would have Max homodimer bound. Displacement and binding of the second (different) monomer to form a heterodimer−DNA complex may serve to aid in selection of DNA. The heterodimer binding affinity to non-E-box DNA is much lower. Therefore, if Max_2−DNA is bound to a less favorable site, the displacement by Myc or Mad may well cause release of the protein. However, it is interesting to observe that the second monomer has much lower affinity for the monomer−DNA than the first monomer binding to DNA (micromolar compared to nanomolar affinity). It is clear from these data that binding of DNA to the Max monomer reduces the affinity for the second monomer. Looked at from the perspective of the Max protein, DNA binding reduces the affinity of Max for its partner protein. This is true whether Max forms heterodimers with Myc or Mad or forms a homodimer with a second Max monomer. Comparing K_2 with K_4, the second monomer is destabilized by 6.2 and 6.8 kJ/mol for Myc-Max or Mad-Max, respectively. These results are somewhat surprising given the stability of the dimer−DNA complex. The destabilization or anticooperative binding may result from the conformational change that monomers are believed to undergo upon binding. The basic region is largely unstructured in solution but folds to an α helix upon binding to DNA. Whether this change occurs on the monomer level or only after the dimer has formed has not been determined. The effects of this conformational change on equilibria may be to destabilize nonspecific interactions. The monomers are believed to have a fast on and off rate. A second monomer association may induce the conformational change which results in a more rigid conformation that interacts more precisely with the E-box. This dimer may have slower on and off rates. The equilibria predict that the binding of the second monomer reduces the site occupancy, but the kinetics may determine the rate of formation of the complex.

The data reported here give new insight into the assembly of protein−DNA scaffolding and support the importance of protein−protein interactions in determining the selection and stability of dimer−DNA complexes. Further interactions of other protein factors such as Mnt and Mxl are likely to alter the stability of these complexes, largely through the protein−protein interactions. Such changes in stability are predicted to be important in regulation of the transcription complex composition and function and are possible targets for therapeutic intervention.

REFERENCES

1. Ferre-D'Amare, A. R., Pognonec, P., Roeder, R. G., and Burley, S. K. (1994) Structure and function of the b/HLH/z Domain of USF, *EMBO J. 13*, 180−189.
2. Ayer, D. E., and Eisenman, R. N. (1993) A switch from Myc: Max to Mad:Max heterocomplexes accompanies monocyte/macrophage differentiation, *Genes Dev. 7*, 2110−2119.
3. Amati, B., Littlewood, T. D., Evan, G. I., and Land, H. (1993) The c-Myc protein induces cell cycle progression and apoptosis through dimerization with Max, *EMBO J. 12*, 5083−5087.
4. Littlewood, T. D., Amati, B., Land, H., and Evan, G. I. (1992) Max and c-Myc/Max DNA-binding activities in cell extracts, *Oncogene 7*, 1783−1792.
5. Carr, C. S., and Sharp, P. A. (1990) A helix-loop-helix protein related to the immunoglobulin E box-binding proteins, *Mol. Cell. Biol. 10*, 4384−4388.
6. Muhle-Goll, C., Nilges, M., and Pastore, A. (1995) The leucine zippers of the HLH-LZ proteins Max and c-Myc preferentially form heterodimers, *Biochemistry 34*, 13554−64.
7. Beckmann, H., and Kadesch, T. (1991) The leucine zipper of TFE3 dictates helix-loop-helix dimerization specificity, *Genes Dev. 5*, 1057−66.
8. Atchley, W. R., and Fitch, W. M. (1995) Myc and Max: molecular evolution of a family of proto-oncogene products and their dimerization partner, *Proc. Natl. Acad. Sci. U.S.A. 92*, 10217−10221.
9. Billin, A. N., Eilers, A. L., Queva, C., and Ayer, D. E. (1999) Mlx, a novel Max-like BHLHZip protein that interacts with the Max network of transcription factors, *J. Biol. Chem. 274*, 36344−36350.
10. Billin, A. N., Eilers, A. L., Coulter, K. L., Logan, J. S., and Ayer, D. E. (2000) MondoA, a novel basic helix-loop-helix-leucine zipper transcriptional activator that constitutes a positive branch of a Max-like network, *Mol. Cell. Biol. 20*, 8845−8854.
11. Hurlin, P. J., Queva, C., and Eisenman, R. N. (1997) Mnt: a novel Max-interacting protein and Myc antagonist, *Curr. Top. Microbiol. Immunol. 224*, 115−121.
12. Askew, D. S., Ashmun, R. A., Simmons, B. C., and Cleveland, J. L. (1991) Constitutive c-myc expression in an IL-3-dependent myeloid cell line suppresses cell cycle arrest and accelerates apoptosis, *Oncogene 6*, 1915−1922.
13. Cole, M. D. (1991) Myc meets its Max, *Cell 65*, 715−716.
14. Evan, G. I., and Littlewood, T. D. (1993) The role of c-myc in cell growth, *Curr. Opin. Genet. Dev. 3*, 44−49.
15. Cerni, C., Bousset, K., Seelos, C., Burkhardt, H., Henriksson, M., and Luscher, B. (1995) Differential effects by Mad and Max on transformation by cellular and viral oncoproteins, *Oncogene 11*, 587−596.
16. Austen, M., Cerni, C., Henriksson, M., Hilfenhaus, S., Luscher-Firzlaff, J. M., Menkel, A., Seelos, C., Sommer, A., and Luscher, B. (1997) Regulation of cell growth by the Myc-Max-Mad network: role of Mad proteins and YY1, *Curr. Top. Microbiol. Immunol. 224*, 123−130.
17. McMahon, S. B., Wood, M. A., and Cole, M. D. (2000) The essential cofactor TRRAP recruits the histone acetyltransferase HGCN5 to cMyc, *Mol. Cell. Biol. 20*, 556−562.
18. Bouchard, C., Dittrich, O., Kiermaier, A., Dohmann, K., Menkel, A., Eilers, M., and Luscher, B. (2001) Regulation of cyclin D2 gene expression by the Myc/Max/Mad network: Myc-dependent TRRAP recruitment and histone acetylation at the cyclin D2 promoter, *Genes Dev. 15*, 2042−2047.
19. Murre, C., McCam, P. S., and Baltimore, D. (1989) A new DNA binding and dimerization motif in immunoglobulin enhancer binding, daughterless, MyoD and Myc proteins, *Cell 56*, 777−783.
20. Amin, C., Wagner, A. J., and Hay, N. (1993) Sequence-specific transcriptional activation by Myc and repression by Max, *Mol. Cell. Biol. 13*, 383−390.
21. Ferre-D'Amare, A. R., Prendergast, G. C., Ziff, E. B., and Burley, S. K. (1993) Recognition by Max of its cognate DNA through a dimeric b/HLH/Z domain, *Nature 363*, 38−45.

22. Nair, S. K., and Burley, S. K. (2003) X-ray structures of Myc-Max and Mad-Max recognizing DNA. Molecular bases of regulation by proto-oncogenic transcription factors, *Cell 112*, 193−205.
23. Prendergast, G. C., Lawe, D., and Ziff, E. B. (1991) Association of Myn, the murine homolog of Max with c-Myc stimulates methylation-sensitive DNA binding and ras cotransformation, *Cell 65*, 395−407.
24. Wechsler, D. S., and Dang, C. V. (1992) Opposite orientations of DNA bending by c-Myc and Max, *Proc. Natl. Acad. Sci. U.S.A. 89*, 7635−7639.
25. Sha, M., Ferre-D'Amare, A. R., Burley, S. K., and Goss, D. J. (1995) Anti-cooperative biphasic equlibrium binding of transcription factor upstream stimulatory factor to its cognate DNA monitored by protein fluorescence changes, *J. Biol. Chem. 270*, 19325−19329.
26. Xu, D., Popov, N., Hou, M., Wang, Q., Bjorkholm, M., Gruber, A., Menkel, A. R., and Henriksson, M. (2001) Switch from Myc/Max to Mad1/Max binding and decrease in histone acetylation at the telomerase reverse transcriptase promoter during differentiation of HL60 cells, *Proc. Natl. Acad. Sci. U.S.A. 98*, 3826−3831.
27. Grandori, C., Cowley, S. M., James, L. P., and Eisenman, R. N. (2000) The Myc/Max/Mad network and the transcriptional control of cell behavior, *Annu. Rev. Cell. Dev. Biol. 16*, 653−699.
28. Hurlin, P. J., Queva, C., and Eisenman, R. N. (1997) Mnt, a novel Max-interacting protein is coexpressed with Myc in proliferating cells and mediates repression at Myc binding sites, *Genes Dev. 11*, 44−58.
29. Hurlin, P. J., Steingrimsson, E., Copeland, N. G., Jenkins, N. A., and Eisenman, R. N. (1999) Mga, a dual-specificity transcription factor that interacts with Max and contains a T-domain DNA-binding motif, *EMBO J. 18*, 7019−7028.
30. Meroni, G., Cairo, S., Merla, G., Messali, S., Brent, R., Ballabio, A., and Reymond, A. (2000) Mlx, a new Max-like bHLHZip family member: the center stage of a novel transcription factors regulatory pathway?, *Oncogene 19*, 3266−3277.
31. Cairo, S., Merla, G., Urbinati, F., Ballabio, A., and Reymond, A. (2001) WBSCR14, a gene mapping to the Williams-Beuren syndrome deleted region, is a new member of the M1x transcription factor network, *Hum. Mol. Genet. 10*, 617−627.
32. Kretzner, L., Blackwood, E. M., and Eisenman, R. N. (1992) Transcriptional activities of the Myc and Max proteins in mammalian cells, *Curr. Top. Microbiol. Immunol. 182*, 435−443.
33. Wechsler, D. S., Papoulas, O., Dang, C. V., and Kingston, R. E. (1994) Differential binding of c-Myc and Max to nucleosomal DNA, *Mol. Cell. Biol. 14*, 4097−4107.
34. Dang, C. V. (1999) c-Myc target genes involved in cell growth, apoptosis, and metabolism, *Mol. Cell. Biol. 19*, 1−11.
35. Amati, B., Dalton, S., Brooks, M. W., Littlewood, T. D., Evan, G. I., and Land, H. (1992) Transcriptional activation by the human c-Myc oncoprotein in yeast requires interaction with Max, *Nature 359*, 423−426.
36. Berberich, S. J., and Cole, M. D. (1992) Casein kinase II inhibits the DNA-binding activity of Max homodimers but not Myc/Max heterodimers, *Genes Dev. 6*, 166−176.
37. Pulverer, B., Sommer, A., McArthur, G. A., Eisenman, R. N., and Luscher, B. (2000) Analysis of Myc/Max/Mad network members in adipogenesis: inhibition of the proliferative burst and differentiation by ectopically expressed Mad1, *J. Cell Physiol. 183*, 399−410.
38. Roussel, M. F., Ashmun, R., Sherr, C., Eisenman, R., and Ayer, D. (1996) Inhibition of cell proliferation by the Mad1 transcriptonal repressor, *Mol. Cell. Biol. 16*, 2796−2801.
39. Lakowicz, J. R. (1983) *Principles of Fluorescence Spectroscopy*, Plenum Publishing Corp., New York.
40. Sha, M., Wang, Y., Xiang, T., van Heerden, A., Browning, K., and Goss, D. J. (1995) Interaction of wheat germ protein synthesis initiation factor eIF-(iso)4F and its subunits p28 and p86 with m7GTP and mRNA analogs, *J. Biol. Chem. 270*, 29904−29909.
41. Kohler, J., and Schepartz, A. (2001) Kinetic studies of Fos-Jun-DNA complex formation: DNA binding prior to dimerization, *Biochemistry 40*, 130−142.
42. Wei, C.-C., Balasta, M. L., Ren, J., and Goss, D. J. (1998) Wheat germ poly(A) binding protein enhances the binding affinity of eukaryotic initiation factor 4F and (iso)4F for cap analogs, *Biochemistry 37*, 1910−1916.
43. Winston, R., and Gottesfeld, J. (2000) Rapid identification of key amino-acid-DNA contacts through combinatorial peptide synthesis, *Chem. Biol. 7*, 245−251.
44. Cave, J. W., Kremer, W., and Wemmer, D. E. (2000) Backbone dynamics of sequence specific recognition and binding by the yeast Pho4 bHLH domain probed by NMR, *Protein Sci. 9*, 2354−2365.
45. Weber, G. (1975) Energetics of ligand binding to proteins, *Adv. Protein Chem. 29*, 2−78.
46. Blackwell, T. K., Huang, J., Ma, A., Kretzner, L., Alt, F. W., Eisenman, R. N., and Weintraub, H. (1993) Binding of myc proteins to canonical and noncanonical DNA sequences, *Mol. Cell. Biol. 13*, 5216−5224.
47. O'Hagan, R. C., Schreiber-Agus, N., Chen, K., David, G., Engelman, J. A., Schwab, R., Alland, L., Thomson, C., Roning, D. R., Scchettini, J. C., et al. (2000) Gene target recognition among members of the Myc superfamily and implications for oncogenesis, *Nat. Genet. 24*, 113−119.
48. Solomon, D. L., Amati, B., and Land, H. (1993) Distinct DNA binding preferences for the c-Myc/Max and Max/Max dimers, *Nucleic Acids Res. 21*, 5372−5376.
49. James, L., and Eisneman, R. (2002) Myc and Mad bHLHZ domains possess identical DNA-binding specificities but only partially overlapping functions *in vivo*, *Proc. Natl. Acad. Sci. U.S.A. 99*, 10429−10434.
50. Park, S., Chung, S., Kim, K.-M., Jung, K.-C., Park, C., Hahm, E.-R., and Yang, C.-H. (2004) Determination of binding constant of transcription factor myc-max/max-max and E-box DNA: the effects of inhibitors on the binding, *Biochim. Biophys. Acta 1670*, 217−228.
51. Blackwood, E. M., Luscher, B., and Eisenman, R. N. (1992) Myc and Max associate in vivo, *Genes Dev. 6*, 71−80.

BI050206I